Materials Science-Poland, Vol. 26, No. 1, 2008

Microstructure and magnetic properties of nanocrystalline Fe-based alloys

M. HASIAK[1*], M. MIGLIERINI[2], J. KALETA[1], J. ZBROSZCZYK[3], H. FUKUNAGA[4]

[1]Institute of Materials Science and Applied Mechanics, Wrocław University of Technology, ul. Smoluchowskiego 25, 50-370 Wrocław, Poland

[2]Department of Nuclear Physics and Technology, Slovak University of Technology, Ilkovičova 3, 812-19 Bratislava, Slovakia

[3]Institute of Physics, Technical University of Częstochowa, al. Armii Krajowej 19, 42-200 Częstochowa, Poland

[4]Faculty of Engineering, Nagasaki University, 852-8521 Nagasaki, Japan

Microstructure and magnetic properties of nanocrystalline $Fe_{82}(Zr_4Nb_3)B_{10}Cu_1$ and $Fe_{80}(Zr_4Mn_3)B_{12}Cu_1$ alloys with different content of the crystalline phase have been investigated. Changes in the microstructure with progressing crystallization were observed by the room temperature Mössbauer spectroscopy. Good soft magnetic properties and frequency characteristics were found in the nanocrystalline $Fe_{82}(Zr_4Nb_3)B_{10}Cu_1$ and $Fe_{80}(Zr_4Mn_3)B_{12}Cu_1$ samples with 50-60% of the crystalline α-Fe phase.

Key words: *amorphous alloy; nanocrystalline alloy; Mössbauer spectroscopy; hysteresis loop; core losses*

1. Introduction

Nanocrystalline Fe–Zr–B–(Cu) alloys patented under the trade name NANOPERM with bcc Fe grains of about 20–30 nm exhibit good soft magnetic properties i.e., high saturation magnetization, low coercivity and good frequency characteristics [1-3] resulting from the presence of fine grains magnetically interacting with each other [4]. Moreover, magnetic properties of nanocrystalline Fe–Zr–B–(Cu) alloys strongly depend on the microstructure of precursors which can be modified by the conditions during the sample preparation. Addition of Nb, Hf, Mn, Ti and other metalloid atoms to the NANOPERM type alloys during fabrication leads to an improvement of their soft magnetic properties [5, 6].

*Corresponding author, e-mail: mariusz.hasiak@pwr.wroc.pl

The aim of this paper is to study effects of Nb and Mn addition on the formation of nanocrystalline structures and magnetic properties of partially crystallized Fe–Zr-(Nb, Mn)–B–Cu alloys.

2. Experimental

Rapidly solidified ribbons of $Fe_{82}(Zr_4Nb_3)B_{10}Cu_1$ and $Fe_{80}(Zr_4Mn_3)B_{12}Cu_1$ alloys were obtained by a single roller melt-spinning method in argon protective atmosphere. The width and thickness of the investigated samples were 2.20 mm and 0.02 mm, respectively. Ribbons in the as-quenched state were partially crystallized which was confirmed by X-ray diffraction using a URD-6 (VEB Carl Zeiss, Jena) diffractometer. The changes in the microstructure were examined at room temperature by the Mössbauer spectroscopy in a transmission geometry using a ^{57}Co source in a Rh matrix. Mössbauer spectra obtained for $Fe_{82}(Zr_4Nb_3)B_{10}Cu_1$ and $Fe_{80}(Zr_4Mn_3)B_{12}Cu_1$ alloys in the as-quenched state and after heat treatment were evaluated by hyperfine field distributions using the NORMOS package program [7]. Isothermal annealing was performed at 773 K and 823 K under the vacuum of about 5×10^{-3} Pa for various time periods. AC and DC magnetic measurements were carried out upon 100 mm long ribbons using a M-H Loop Tracer (Tesla) and equipment for magnetic measurements MMS-4001 (Ryowa Electronics).

3. Results and discussion

Precursors of $Fe_{82}(Zr_4Nb_3)B_{10}Cu_1$ and $Fe_{80}(Zr_4Mn_3)B_{12}Cu_1$ alloys were partially crystallized already in the as-quenched state as confirmed by X-ray diffractometry and Mössbauer spectroscopy. X-ay diffraction patterns show narrow peaks corresponding to the crystalline α-Fe phase superimposed upon a broad amorphous reflection. Mössbauer spectra of as-quenched (a.q.) and annealed $Fe_{82}(Zr_4Nb_3)B_{10}Cu_1$ and $Fe_{80}(Zr_4Mn_3)B_{12}Cu_1$ alloys are shown in Fig. 1 together with their spectral components. Corresponding hyperfine field distributions $P(B)$ are drawn alongside each spectra. The spectra consist of broad, overlapped lines assigned to disordered structural positions of resonant atoms, whereas sharp narrow lines indicate a presence of bcc-Fe crystallites. The experimental data were fitted by separate independent blocks of hyperfine field distributions and a sextet of Lorentzian lines using the NORMOS package program.

Magnetic properties of the NANOPERM type alloys strongly depend on their microstructure [8, 9]. Both investigated samples of $Fe_{82}(Zr_4Nb_3)B_{10}Cu_1$ and $Fe_{80}(Zr_4Mn_3)B_{12}Cu_1$ alloys show rather poor soft magnetic properties in the as quenched states. Dependences of magnetic flux densities on magnetic field obtained for the investigated samples are presented in Fig. 2 in the form of magnetic hysteresis loops. The as-quenched Nb- and Mn-containing ribbons exhibit the saturation magnetic flux density (B_s) of about 1.3 T and 1.0 T, respectively. The coercivity (H_c) of the as-quenched $Fe_{80}(Zr_4Mn_3)B_{12}Cu_1$

alloy is equal to 30 A/m being three times lower than that of the $Fe_{82}(Zr_4Nb_3)B_{10}Cu_1$ alloy. Upon increasing annealing temperature up to 823 K ($Fe_{82}(Zr_4Nb_3)B_{10}Cu_1$) and 773 K ($Fe_{80}(Zr_4Mn_3)B_{12}Cu_1$), an increase of B_s and decrease of H_c for both investigated samples is observed. The maximum saturation magnetic flux density of about $B_s = 1.6$ T was achieved for the Mn-containing ribbon annealed at 773 K for 0.5 h, and $B_s = 1.4$ T was found for the Nb-containing ribbon annealed at 823 K for 0.5 h. Furthermore, optimum annealing conditions lead to a decrease in the coercivity

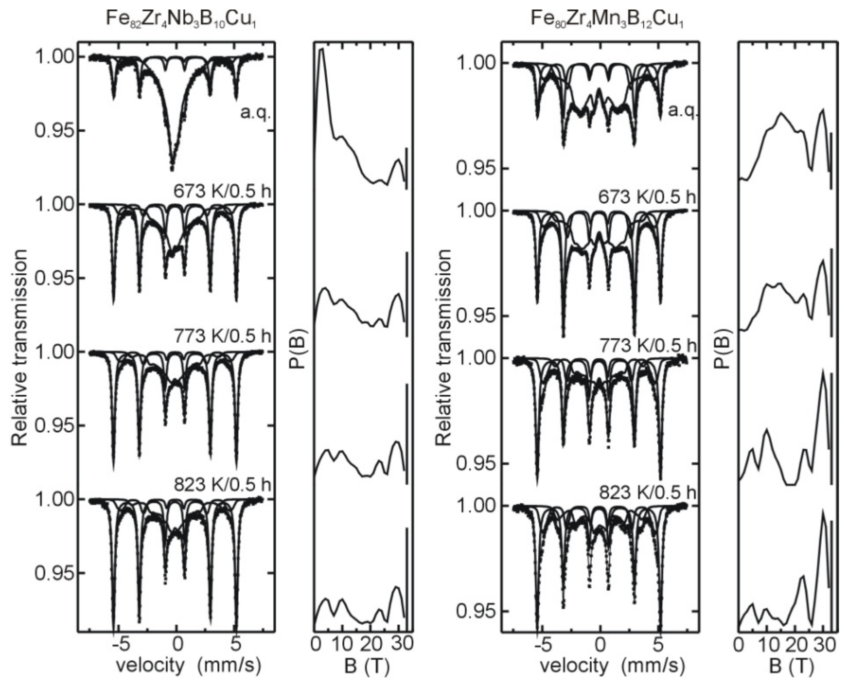

Fig. 1. Mössbauer spectra and hyperfine field distributions of the $Fe_{82}(Zr_4Nb_3)B_{10}Cu_1$ and $Fe_{80}(Zr_4Mn_3)B_{12}Cu_1$ alloys

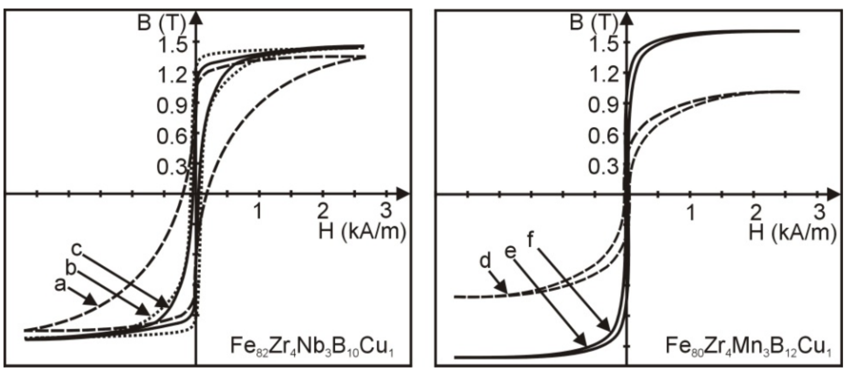

Fig. 2. DC hysteresis loops for the $Fe_{82}(Zr_4Nb_3)B_{10}Cu_1$ (a, b, c) and $Fe_{80}(Zr_4Mn_3)B_{12}Cu_1$ (d, e, f) alloys in the as-quenched state (a, d) and after 0.5 h annealing at 773 K (b, e) and 823 K (c, f)

to 40 A/m and 20 A/m for the $Fe_{82}(Zr_4Nb_3)B_{10}Cu_1$ and $Fe_{80}(Zr_4Mn_3)B_{12}Cu_1$ alloys, respectively. DC hysteresis loops obtained for the $Fe_{80}(Zr_4Mn_3)B_{12}Cu_1$ alloy after 0.5 h annealing at 773 K and 823 K are almost identical (Fig. 2, curves e and f).

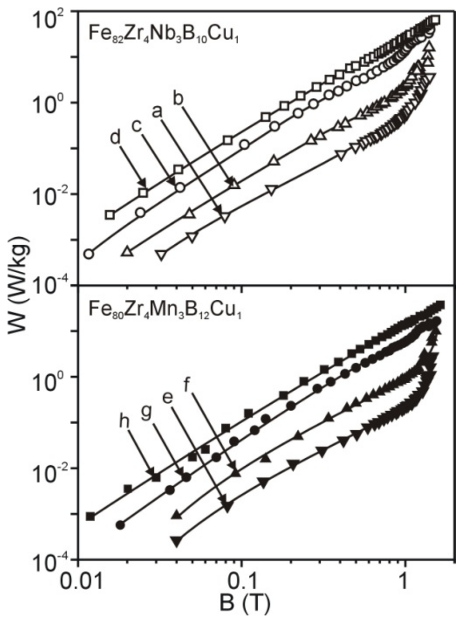

Fig. 3. Dependences of core losses (W) on induction (B) for the $Fe_{82}(Zr_4Nb_3)B_{10}Cu_1$ alloy (a, b, c, d) and $Fe_{80}(Zr_4Mn_3)B_{12}Cu_1$ alloy (e, f, g, h) after 0.5 h annealing at 823 K and 773 K, respectively, measured at the frequency of 50 Hz (a, e), 200 Hz (b, f), 1 kHz (c, g), and 2 kHz (d, h)

AC magnetic properties of the investigated alloys annealed at optimum conditions are presented in Fig. 3 as dependences of core losses (W) on magnetic induction (B) for various frequencies. The core losses monotonically increase with induction for all investigated samples. In addition, the core losses of both samples are higher with increasing frequency of measurement due to eddy currents. The sample with Mn exhibits systematically lower values of W than the one with Nb.

Dependences of the effective permeability (μ_e) and the loss factor $\tan\delta$ upon the magnetic field H are plotted in Figs. 4 and 5, respectively ($\tan\delta = \mu''/\mu'$; the real (μ') and imaginary (μ'') parts of permeability express the components of the induction B which are in phase with the magnetic field H and delayed by the phase angle of 90º from H, respectively [10]). The effective permeability measured at the frequency of 250 Hz increases for all investigated samples to its maximum at the magnetic field range 45–55 A/m and then decreases (Fig. 4). The maximum value of μ_e for the Nb -containing sample is shifted towards higher magnetic fields than that of the Mn -containing sample. The increase of the maximum effective permeability up to 13 000 and 9200 after 0.5 h annealing of the $Fe_{80}(Zr_4Mn_3)B_{12}Cu_1$ alloy at 773 K and the $Fe_{82}(Zr_4Nb_3)B_{10}Cu_1$ at 823 K is connected with an irreversible structural relaxation during the heat treatment process. It is worth noting that the effective permeability does not show appreciable deviations from those presented in the figure in a wide range of the measuring frequencies up to few kHz.

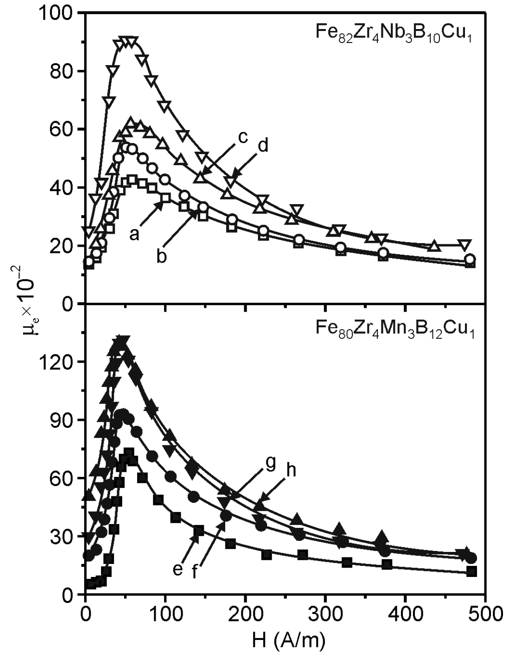

Fig. 4. Effective permeability (μ_e) vs. magnetic field (H) for the $Fe_{82}(Zr_4Nb_3)B_{10}Cu_1$ (a, b, c, d) and $Fe_{80}(Zr_4Mn_3)B_{12}Cu_1$ (e, f, g, h) alloys in the as-quenched state (a, e) and annealed at 673 K (b, f), 773 K (c, g) and 823 K (d, h) for 0.5 h measured at the frequency of 250 Hz

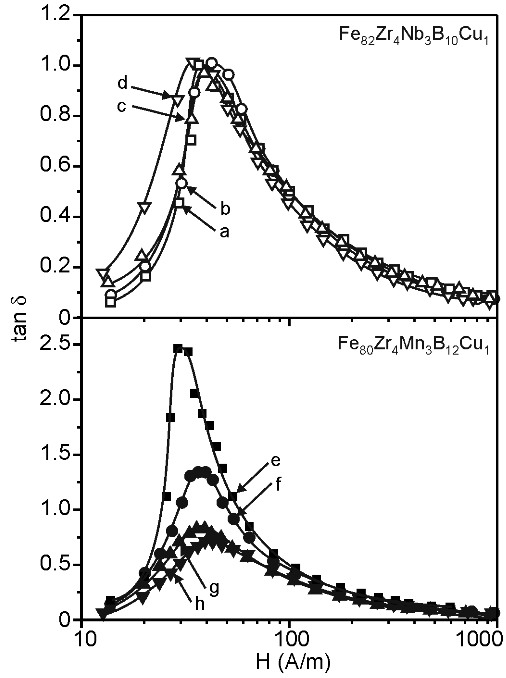

Fig. 5. Dependences of the loss factor (tanδ) on magnetic field (H) at f = 250 Hz for the $Fe_{82}(Zr_4Nb_3)B_{10}Cu_1$ (a, b, c, d) and $Fe_{80}(Zr_4Mn_3)B_{12}Cu_1$ (e, f, g, h) alloys in the as quenched state (a, e) and annealed for 0.5 h at 673 K (b, f), 773 K (c, g) and 823 K (d, h)

Dependences of the loss factor tanδ on the magnetic field (Fig. 5) for the both alloys exhibit a similar behaviour as the effective permeabilities. The loss factor of the as-quenched sample with Mn is two times higher than that of the $Fe_{82}(Zr_4Nb_3)B_{10}Cu_1$ alloy. After annealing, the values of tanδ are similar for both investigated samples. It should be noted that the maximum loss factors were obtained at lower magnetic fields than the maximum effective permeability.

4. Conclusions

The results of magnetic measurements for the nanocrystalline $Fe_{82}(Zr_4Nb_3)B_{10}Cu_1$ and $Fe_{80}(Zr_4Mn_3)B_{12}Cu_1$ alloys with various amounts of the crystalline phases have been reported. Nanocrystalline alloys with the bcc grain fraction higher than 50% of the sample volume exhibit good soft magnetic properties. Nb and Mn-containing samples show the maximum permeabilities of 9200 and 13 000, respectively, at the magnetic field of about 50 A/m. Moreover, the ribbons of the $Fe_{82}(Zr_4Nb_3)B_{10}Cu_1$ and $Fe_{80}(Zr_4Mn_3)B_{12}Cu_1$ alloys annealed at 773 K and 823 K show low core losses which increase with the frequency of measurement.

Acknowledgements

This work was supported by the grants PBZ/MEiN/01/2006/09 (M. Hasiak) and VEGA 1/4011/07, APVT 20-008404 (M. Miglierini).

References

[1] SUZUKI K., KATAOKA N., INOUE A., MAKINO A., MASUMOTO T., Mater. Trans. JIM, 31 (1990), 743.
[2] MAKINO A., BITOH T., INOUE A., MASUMOTO T., J. Appl. Phys., 81 (1997), 2736.
[3] MAKINO A., BITOH T., KOJIMA A., INOUE A., MASUMOTO T., Mater. Sci. Eng. A, 304-306 (2001), 1083.
[4] SUZUKI K., HERZER G., CADOGAN J.M., J. Magn. Magn. Mater., 177–181 (1998), 949.
[5] MÜLLER M., GRAHL H., MATTERN N., KÜHN U., Mater. Sci. Eng. A, 226-228 (1997), 565.
[6] SUZUKI K., MAKINO A., KATAOKA N., INOUE A., MASUMOTO T., Mater. Trans. JIM, 32 (1991), 93.
[7] BRAND R.A., *NORMOS program*, Universität Duisburg, 1999.
[8] VARGA L.K., LOVAS A., POGÁNY L., KISS L.F., BALOGH J., KEMÉNY T., Mater. Sci. Eng. A, 226–228 (1997), 740.
[9] HASIAK M., MIGLIERINI M., YAMASHIRO Y., CIURZYŃSKA W.H., FUKUNAGA H., J. Magn. Magn. Mater., 239 (2002), 506.
[10] CHIKAZUMI S., *Physics of Ferromagnetism*, Clarendon Press, Oxford, 1997.

Received 28 April 2007
Revised 16 February 2008